View metadata, citation and similar papers at core.ac.uk
brought to you by CORE
provided by Repositorio da Producao Cientifica e Intelectual da Unicamp

Aligned pipe arrays formation by silicon anodic etching

M. C. dos Santos and O. Teschke

Citation: Journal of Vacuum Science & Technology B **16**, 2105 (1998); doi: 10.1116/1.590136
View online: http://dx.doi.org/10.1116/1.590136
View Table of Contents: http://scitation.aip.org/content/avs/journal/jvstb/16/4?ver=pdfcov
Published by the AVS: Science & Technology of Materials, Interfaces, and Processing

Articles you may be interested in
Silicon nanoparticle formation by short pulse electrochemical etching in the transition regime
J. Appl. Phys. **100**, 104307 (2006); 10.1063/1.2384809

Mechanism of a remarkable enhancement in the light emission from nanocrystalline porous silicon annealed in high-pressure water vapor
J. Appl. Phys. **98**, 123509 (2005); 10.1063/1.2147847

Self-ordered pore structure of anodized aluminum on silicon and pattern transfer
Appl. Phys. Lett. **76**, 49 (2000); 10.1063/1.125652

Enhancement of the quantum efficiency and stability of electroluminescence from porous silicon by anodic passivation
Appl. Phys. Lett. **73**, 2021 (1998); 10.1063/1.122355

Control of silicon nanocrystallite shape asymmetry and orientation anisotropy by light-assisted anodization
Appl. Phys. Lett. **70**, 1116 (1997); 10.1063/1.118502

Instruments for Advanced Science

Contact Hiden Analytical for further details:
W www.HidenAnalytical.com
E info@hiden.co.uk
CLICK TO VIEW our product catalogue

Gas Analysis
- dynamic measurement of reaction gas streams
- catalysis and thermal analysis
- molecular beam studies
- dissolved species probes
- fermentation, environmental and ecological studies

Surface Science
- UHV TPD
- SIMS
- end point detection in ion beam etch
- elemental imaging - surface mapping

Plasma Diagnostics
- plasma source characterization
- etch and deposition process reaction
- kinetic studies
- analysis of neutral and radical species

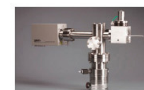
Vacuum Analysis
- partial pressure measurement and control of process gases
- reactive sputter process control
- vacuum diagnostics
- vacuum coating process monitoring

Redistribution subject to AVS license or copyright; see http://scitation.aip.org/termsconditions. Download to IP: 143.106.1.143 On: Fri, 15 Aug 2014 16:48:45

Aligned pipe arrays formation by silicon anodic etching

M. C. dos Santos and O. Teschke[a)]
Nano-structure Laboratory, Instituto de Física, UNICAMP, Caixa Postal 6165, 13081-970, Campinas, SP, Brazil

(Received 14 August 1997; accepted 15 May 1998)

A simple technique is described here that produces aligned curved or straight arrays of pipes. This opens the way to produce complete systems (electronic, photonic and fiber optic connectors) from silicon with large scale fabrication techniques. Our strategy in creating parallel pipes is to use high current densities (~100 mA/cm^2) silicon anodization in HF solutions, in a cell where the current direction and the preferential etching directions are not coincident in (111) silicon substrates. The etched structure in a nanoscale range was observed using atomic force microscopy, which shows steps. In a macroscopic scale steps were observed in the walls of arrays of tenths of millimeters diameter pipes. Pores arrays were obtained forming a ~90° angle with the current direction. Molecular mechanics simulations of the pipe wall structure show that a preferential etching along the ⟨100⟩ direction and passivation of the (111) planes are the mechanisms responsible for the formation of pore arrays structure. © *1998 American Vacuum Society.* [S0734-211X(98)07404-6]

I. INTRODUCTION

Silicon etched structures are becoming increasingly important due to the prospect of producing fully integrated electronic devices.[1] The study of the properties of these structures is essential to control material fabrication processes. In this article we will show that, during porous silicon formation by anodization of silicon in HF solutions, arrays of microchannels may be formed by increasing the silicon etching velocity. This opens the way to produce complete systems (electronic, photonic and fiber optic connectors) from silicon with large scale fabrication techniques.

Pore formation in silicon is a result of electrochemical anodization in hydrofluoric acid solutions. The first reports of silicon etching in HF solutions were published by Uhlir[2] in 1956 and Turner[3] in 1958 who observed color changes of the silicon surface as a result of the etching process. Subsequently, Theunissen[4] showed that the interference colors were due to the formation of a porous structure within the silicon substrate. At current densities approaching the electropolishing regime, the pores are elongated, forming pipes. Pipe formation in *n*-type silicon anodically biased in the dark has been described by Theunissen *et al.*[4–6] The resulting channels are needle-shaped and strongly branched. Lehmann and Foll [7] have detailed the different types of ''pipe'' geometries which occur under different anodization conditions, and have explained ''piping'' in terms of the diffusion of holes to the silicon surface.

Since anodic biasing of *n*-type silicon always creates a space-charge region (depletion),[8] trench formation occurs spontaneously even at polished surfaces.[4–6] The situation is diverse for the *p*-type material. Since the silicon is positively polarized, there is no depletion layer but an accumulation layer. Consequently, a different mechanism has to be responsible for pipe formation.

In this article, we report atomic force microscopy (AFM) and optical microscopy images which reveal the formation of arrays of curved pipes in etched silicon, as well as straight arrays, which were fabricated at 45° and 90° with the silicon slab surface orientation. We will show that the hydrogen generated by the silicon dissolution reaction as a by-product prevents the pore wall dissolution by fluorine atoms. This is demonstrated by simulating the pore formation mechanism using molecular mechanics calculations

II. EXPERIMENT

The electrochemical cell was made of PTFE, with a rectangular cross section (32×65 mm^2). The counter electrode was a circular platinum mesh with a diameter of 35 mm. Three types of samples were prepared such that the surfaces exposed to anodization were different, according to the following procedures: (i) Fig. 1 shows a (111) silicon 5 mm disk from where ~1 mm thick slices were cut, as indicated, to produce samples A ({010} surfaces) and B ({211} surfaces); and (ii) 2 mm thick with 5 cm diameter (111) oriented silicon wafers were usually cut into 4×20 mm rectangular slabs (samples C), although other sizes were also used. Each silicon slab was mounted perpendicularly to the electrolyte level and contact was made near the edge of the wafer. Only the lower part of the wafer was immersed in the solution. A Teflon coated magnetic stirrer was used to keep the solution well mixed, and also to assist in removing bubbles which accumulate on the wafer surface. A detailed account of the sample preparation technique has been previously described.[9,10] The anodization was carried out in 25% HF solutions using a EGG/PAR 273A galvanostat/potentiostat. Optical microscopic observations were made using a Zeiss Axioplan optical microscope and AFM images were taken in a TopoMetrix TMX-2000 microscope.

III. RESULTS AND DISCUSSION

Porous silicon is obtained at low current densities when high resistivity samples (~1–10 Ω cm) are etched.[11] The

a)Electronic mail: oteschke@ifi.unicamp.br

Redistribution subject to AVS license or copyright; see http://scitation.aip.org/termsconditions. Download to IP: 143.106.1.143 On: Fri, 15 Aug 2014 16:48:45

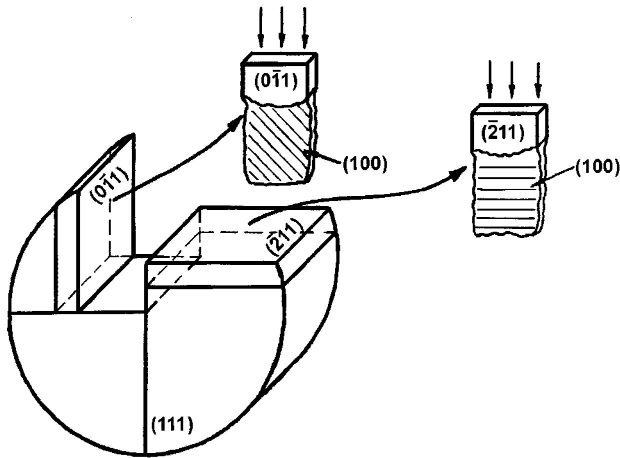

FIG. 1. Schematic diagram showing the crystal orientation and how samples were cut from the silicon wafer. Sample planes exposed to corrosion are indicated.

morphology of a structure formed by applying a low anodic current density to these samples is an interconnected skeleton of nanowires having diameters as small as ~2 nm.[10] It is also generally known that at low current densities the pores are randomly directed in the porous silicon layer. For 0.006 Ω cm silicon, there is neither a microporous layer nor pipe formation when the samples are anodized at low current densities; instead, terraces are formed. Figure 2 shows an AFM image obtained from sample C (0.006 Ω cm), where the exposed surface is (111) oriented, anodized for 5 min at a current density of 5 mA/cm^2. A structure of terraces with ~20 Å steps is observed. Since the AFM tip radius of curvature is ~35 Å, the observed image is the convolution of the etched structure and the tip, which precluded a determination of the angle between the terraces.

A macroscopic observation of the etched structure is then performed. Pore growth was induced by a pattern of pits

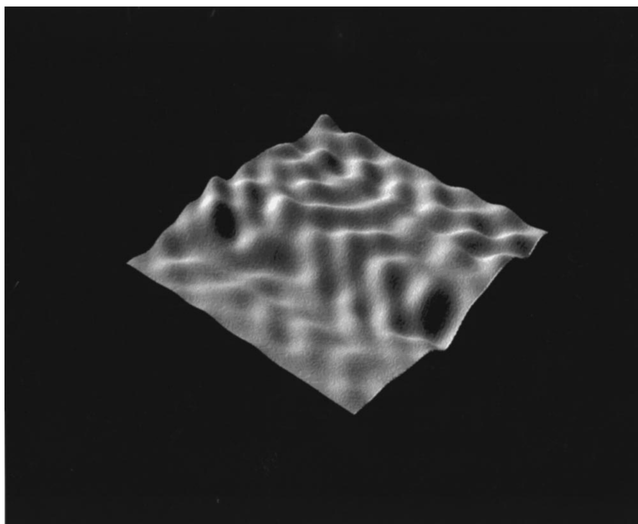

FIG. 2. AFM image of (111)-oriented silicon sample anodized 5 min at 5 mA/cm^2. A 138 Å length is displayed in the x and y directions and 90 Å in the z direction.

produced by cutting the sample surface with a diamond-edged cutter. After pipe array formation the slab is sliced by a razor blade and its internal surface is observed. Figure 3(a) shows a region where there are pipes in a typical p-type 0.006 Ω cm silicon (sample A) formed at high current densities (100 mA/cm^2). The current direction is in the plane of the photograph and it is not coincident with a ⟨100⟩ preferential etching direction. Arrays of parallel pipes at an angle of 45° with slab axis direction is observed.

Similar structures were also obtained tilted at 90° angle with the slab axis direction by simply cutting the silicon slice as in sample B, where the (211) surface is exposed. Figure 3(b) is a 250× optical view of a sliced slab.

Figure 3(c) shows an array of curved pipes obtained for a sample cut at a nonorthogonal direction with the ⟨111⟩ direction (sample C). It shows pipes with different radius of curvature and various diameters. Figure 3(d) shows an array of pipes where the walls have steps that form an angle of ~70° between them. From these results it is concluded that the diameter distribution of straight etched pipes is almost uniform. The diameter depends on the initial position of the pit in the random pit pattern generated by edge cutting the wafer into a rectangular shape. After 10 min anodization time of the original pit distribution only a few percent survived.

In order to understand the pipe formation it is necessary to deal with the mechanism of the anodic surface dissolution. Although the detailed mechanism is still not clear, it probably occurs as follows: At the onset of the anodic current the silicon surface is all H-covered.[12,13] A field built up across the space-charge layer, moves holes towards the surface at kinks, defects or tensioned regions. This induces a nucleophilic attack on the Si–H bonds by F^- [or HF_2^- (Ref. 3)] ions, forming SiF_2 groups at these sites and H^+ ions in the solution. The Si–Si back bonds of the SiF_2 groups are stretched due to the fluorine electronegativity allowing the insertion of F^- (or HF_2^-) ions. The reaction detaches the SiF_2 group from the surface into the solution, and forms two new Si–F bonds which react again as

$$[\mathrm{Si}_N]\mathrm{SiF}_2 + 2h^+_{\mathrm{sol}} + 2F^-_{\mathrm{sol}} \rightarrow [\mathrm{Si}_{N-1}]\mathrm{SiF}_2 + (\mathrm{SiF}_2)_{\mathrm{sol}}. \quad (1)$$

This changes the surface geometry and the electric field distribution so that the next hole transference will preferentially occur at this location thus enlarging the ''pore'' (see Fig. 4). Equation (1) describes the silicon dissolution reaction (SDR). The intermediary product SiF_2 reacts rapidly with HF, forming H_2 and SiF_4 (Ref. 14):

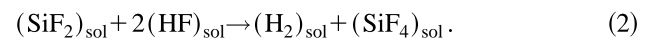

$$(\mathrm{SiF}_2)_{\mathrm{sol}} + 2(\mathrm{HF})_{\mathrm{sol}} \rightarrow (\mathrm{H}_2)_{\mathrm{sol}} + (\mathrm{SiF}_4)_{\mathrm{sol}}. \quad (2)$$

The H_2 oxidation reaction, which occurs at the Si–H surface bonds covering the electrode surface, is given by[13]

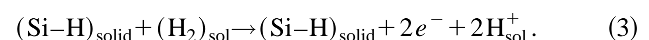

$$(\mathrm{Si{-}H})_{\mathrm{solid}} + (\mathrm{H}_2)_{\mathrm{sol}} \rightarrow (\mathrm{Si{-}H})_{\mathrm{solid}} + 2e^- + 2\mathrm{H}^+_{\mathrm{sol}}. \quad (3)$$

This oxidation of H_2 fixes the electrode potential at a value which prevents its dissolution by fluoride ions.[14] This

Redistribution subject to AVS license or copyright; see http://scitation.aip.org/termsconditions. Download to IP: 143.106.1.143 On: Fri, 15 Aug 2014 16:48:45

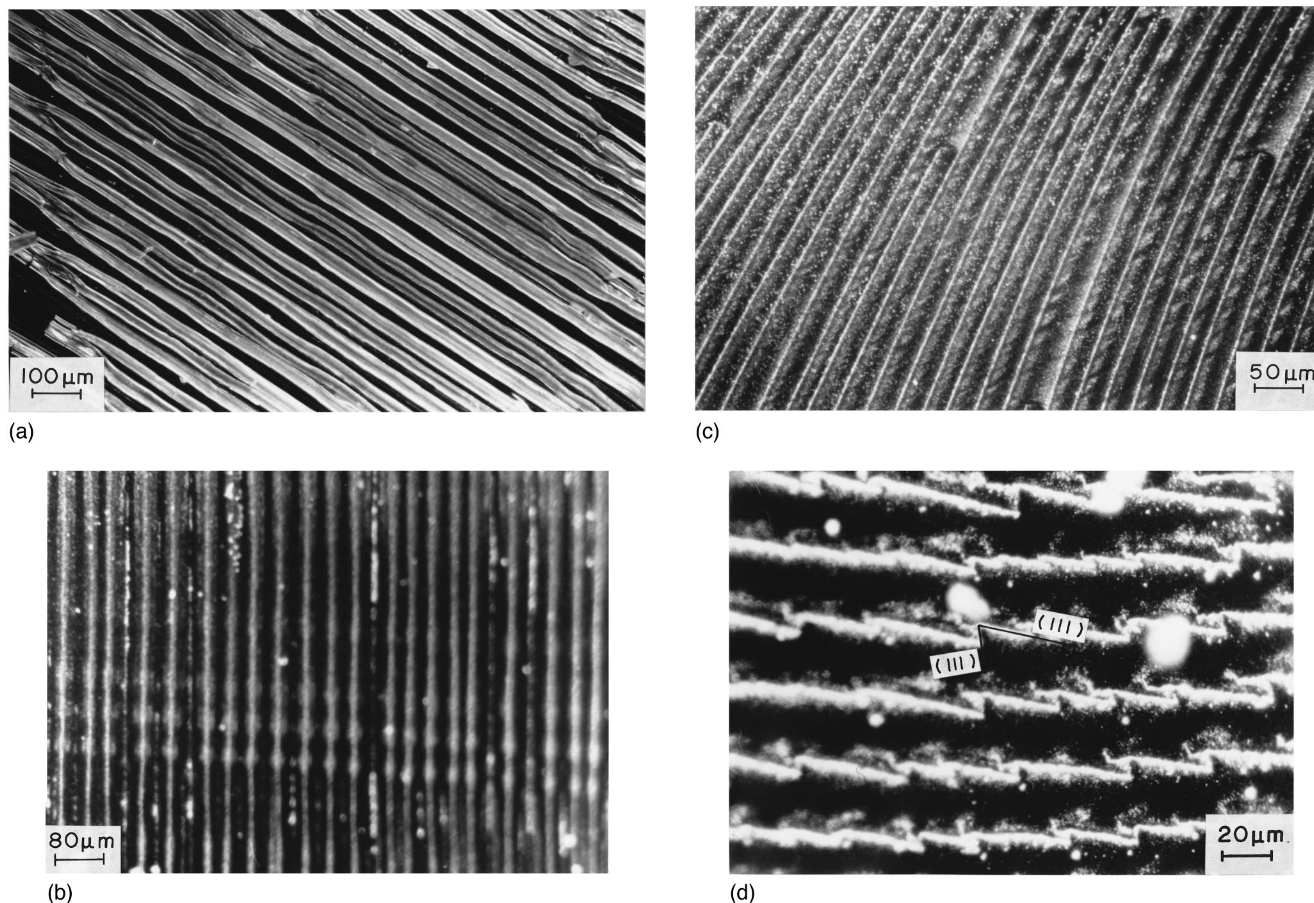

FIG. 3. Array of parallel pipes etched at a current density of ~200 mA/cm^2. (a) Array of pipes at an angle of 45° with the (111) edges (sample A); (b) array of pipes at an angle of 90° with the (011) edges (sample B); (c) array of curved pipes (sample C); (d) array of pipes showing stepped walls formed by the intersection of (111) silicon planes.

is illustrated in Fig. 4. It also displays the schematic distribution of the electric field lines which leads to pipe formation.

Previous work on pipe formation in *n*-type silicon concluded that the space-charge region itself protects the pipe walls from being etched as follows:[7] If all minority carriers are collected by the pipe tips there are none left to permit etching of the wall. This means that a depletion effect is the reason for pipe formation, not an inhibition layer of a different chemical composition at the pipe walls. Here we report on pipe formation in *p*-type material; since the silicon is positively polarized there is no depletion layer and consequently we propose a different mechanism for pipe formation. The hydrogen covered silicon surface (Si–H bonds) which forms the lateral walls of the pipes is passivated by the hydrogen oxidation reaction (H_2 released at the reaction sites) which injects charges into the H-covered sites, preventing wall dissolution by fluorine atoms and increasing the dissolution rate at the bottom of the pipe to where the injected charges migrate. The observed doping dependence of the pipe formation is due to a complex interplay of the silicon dissolution reaction [Eq. (1)] on the dopant concentration, and its by-product reaction [Eq. (2)]. The molecular hydrogen concentration on the H-covered sites then play an important role in the rate of the dissolution reaction at the pore bottoms.

A second effect to be considered is the ability of hydrogen to interact with structural defects and impurities present in the silicon lattice. In particular it has been found that, in crystalline silicon, all the acceptors were passivated by hydrogen, causing a dramatic increase in the resistivity of *p*-type material.[15] This effect adds to the passivation effect produced by hydrogen at the pore walls.

Guided by these results, we performed a large cluster calculation including typically 1000–2000 silicon atoms at the molecular mechanics level. These calculations were carried out within Cerius,[2] a program developed by Molecular Simulations Incorporated, and the universal force field parametrization[16] has been adopted. Conformations obtained were in agreement with our previous AM1 geometry optimization.[13]

Enthalpies of reaction of the cluster with HF were found to be very much dependent on the local symmetry around the silicon atom involved in the reaction. The main conclusions could be summarized as follows: Electrochemical dissolution of silicon in concentrated hydrofluoric acid solutions involves the reaction of Si with HF. Once $>SiF_2$ species are formed at the surface, Si–Si back bonds weaken and SiF_2

Redistribution subject to AVS license or copyright; see http://scitation.aip.org/termsconditions. Download to IP: 143.106.1.143 On: Fri, 15 Aug 2014 16:48:45

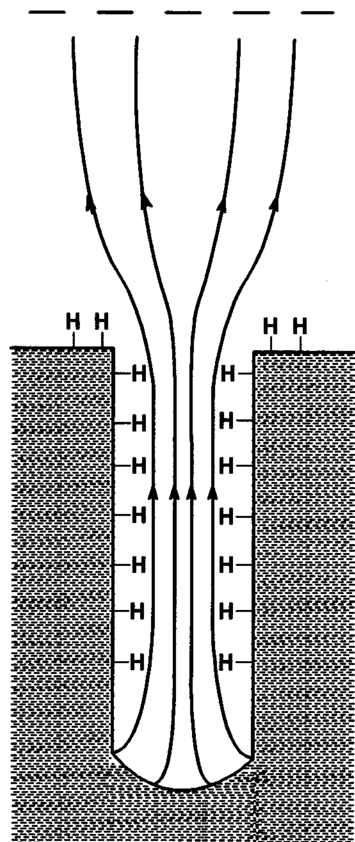

FIG. 4. Schematic diagram of pipe formation mechanism showing the distribution of the electric field lines and the H-covered wall passivated by the hydrogen oxidation reaction.

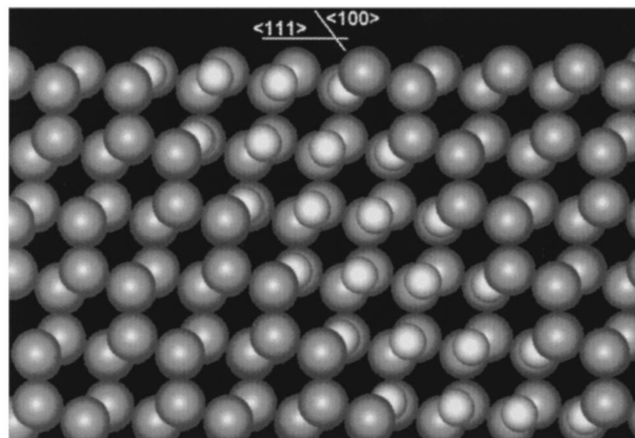

(a)

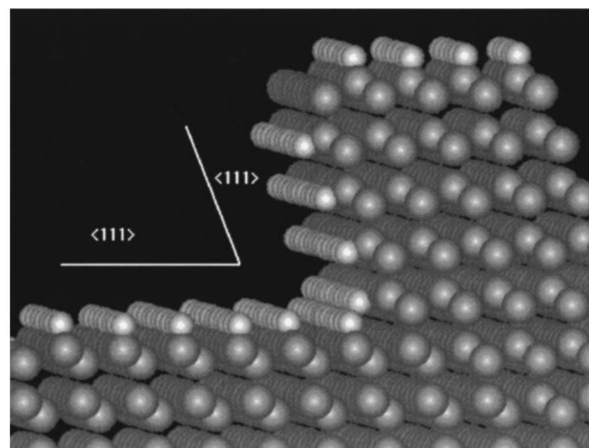

(b)

FIG. 5. Molecular mechanics simulations of the pore walls: (a) transversal section of a small straight pipe forming an angle of 54.7° with the (111) silicon surface and (b) lateral view of a stepped wall that gives rise to curved pipes. The step is formed by intersecting (111) planes, at an angle of 70.5°. Dark and light gray spheres represent hydrogen and silicon atoms, respectively.

molecules separate from the substrate to the solution to further react with HF, producing SiF_4 and H_2.[15] Reaction enthalpies calculated on model clusters at the AM1 level showed that silicon atoms at the (111) surface are much more stable than those at the (100) surface. The energy released in the formation of a SiF_2 fragment on a (111) surface is 14.0 kcal/mol and this reaction requires a high activation energy step which is the breaking of a Si–Si bond. On the other hand, no Si–Si bond cleavage is needed to create such a fragment on a (100) surface, and the energy release obtained in this case is 37.0 kcal/mol. This means that the dissolution reaction tends to follow a path that is determined by the easy direction of etching (atoms along the $\langle 100 \rangle$ direction), and that the exposure of distinct silicon surfaces should determine different patterns of pores at the electrode surface.

Slices oriented as samples A and B have been graphically obtained by faceting a silicon crystal through the planes (111), (211) and (011). A slice having (111) and (211) plane edges, as in sample A, has the $\langle 100 \rangle$ direction forming an angle of 45° with the edges while in a slice having (111) and (011) plane edges, as in sample B, the $\langle 100 \rangle$ direction is perpendicular to the (011) plane. These simple geometrical arguments suggest that samples prepared in this way, as shown in Figs. 3(a) and 3(b), would present pipes at 45° and 90° with the edges if one assumes that pipe growing follows the $\langle 100 \rangle$ direction.

Figure 5(a) shows the optimized structure of the transversal section of the smallest pipe that could be built starting from a (111) surface and following the path given by the $\langle 100 \rangle$ direction. This procedure leaves singly hydrogenated silicon atoms at the pipe walls. This tube is cylindrical in shape, with the axis forming an angle of 54.7° with the (111) surface. Figure 5(b) shows another pipe wall involving a step formed by different (111) planes, which resulted in an angle of 70.5° between them. These structures are in agreement with the ones observed in Figs. 2 and 3. It is also interesting to notice that the intersection of (111) surfaces leaves silicon atoms at the corners that are connected to two other silicon atoms in the wall, that is, in a symmetry similar to the one at the (100) surface. Further fluorine attack on the walls should proceed through these atoms until another step is found.

The high current density ($\sim$100 mA/cm^2) anodization process described in this article results in an array of straight parallel pipes with an almost uniform distribution of diameters. Since the silicon slabs used were (111) oriented, their lateral walls have a different orientation and consequently

Redistribution subject to AVS license or copyright; see http://scitation.aip.org/termsconditions. Download to IP: 143.106.1.143 On: Fri, 15 Aug 2014 16:48:45

the attack takes place preferentially at the plate lateral walls. The pore pattern was produced by cutting the wafers with a diamond-edge cutter. When the current direction is not aligned with the ⟨100⟩ direction the pipes are not aligned with the current, and the etching will proceed in the ⟨100⟩ direction until the etch front hits the {111} planes. The pore walls are consequently {111} planes. In Fig. 3(b), pores follow preferentially the direction normal to the current direction in the plane of the photograph, while Fig. 3(a) has pores preferentially aligned at 45° with the current direction.

Regions of small radius of curvature of the aligned pipes results in the decomposition of the curved pipe walls into the two (111) planes forming an angle of 70.5° between then. This is shown in Fig. 3(d). These pore stepped walls are formed by etching various (100) planes and the remaining structure is formed by the more slowly etched (111) planes.

Figures 3(a) and 3(b) also show that the symmetry of the exposed silicon surface may lead to pipes in any direction, i.e., pipe formation with any orientation or radius of curvature, down to crystallographic steps, may be possible by step etching along the ⟨100⟩ etching directions forming an array of pores with (111) walls.

IV. CONCLUSIONS

In this article we present experimental results showing that silicon slab anodization in HF solution forms arrays of straight or curved parallel pipes. The proposed mechanisms of pipe formation are a preferential etching along the ⟨100⟩ directions and a preferential hydrogen passivation of the (111) planes, in agreement with the observation that during the etching process we may obtain walls formed by (100) and (111) planes. Molecular mechanics simulations of the pipe wall structure give further support for these mechanisms.

ACKNOWLEDGMENTS

The authors are grateful to J. R. Castro and L. O. Bonugli for technical assistance. This work was supported in part by FAPESP 96/4431-9, FINEP and CNPq Grant No. 523.268/95-5.

[1] K. D. Hirschman, L. Tsybeskov, S. P. Duttagupta, and P. M. Fauchet, Nature (London) **384**, 338 (1996).
[2] A. Uhlir, Bell Syst. Tech. J. **35**, 333 (1956).
[3] D. R. Turner, J. Electrochem. Soc. **105**, 402 (1958).
[4] M. J. J. Theunissen, J. Electrochem. Soc. **119**, 351 (1972).
[5] M. J. J. Theunissen, J. A. Appels, and W. H. C. G. Verkuylen, J. Electrochem. Soc. **117**, 959 (1970).
[6] M. J. Hill, J. Electrochem. Soc. **120**, 1425 (1973).
[7] V. Lehmann and H. Foll, J. Electrochem. Soc. **137**, 653 (1990).
[8] S. M. Sze, in *Physics of Semiconductor Devices* (Wiley, New York, 1969).
[9] O. Teschke, M. C. Gonçalves, and F. Galembeck, Appl. Phys. Lett. **63**, 1348 (1993).
[10] O. Teschke, Appl. Phys. Lett. **68**, 2129 (1996).
[11] O. Teschke, F. Alvarez, L. R. Tessler, and M. U. Kleinke, Appl. Phys. Lett. **63**, 1927 (1993).
[12] G. W. Trucks, K. Raghavachari, G. S. Higashi, and Y. J. Chabal, Phys. Rev. Lett. **65**, 504 (1990).
[13] D. M. Soares, M. C. dos Santos, and O. Teschke, Chem. Phys. Lett. **242**, 202 (1995).
[14] D. M. Soares, O. Teschke, and M. C. Santos, Langmuir **12**, 2875 (1996).
[15] S. J. Pearton, W. L. Hansen, E. E. Haller, and J. M. Kahn, J. Appl. Phys. **55**, 1221 (1984).
[16] A. K. Rappé, C. J. Casewit, K. S. Colwell, W. A. Goddard, and W. M. Skiff, J. Am. Chem. Soc. **114**, 10024 (1992).

Redistribution subject to AVS license or copyright; see http://scitation.aip.org/termsconditions. Download to IP: 143.106.1.143 On: Fri, 15 Aug 2014 16:48:45